

STATUS ON NHa C400 CYCLOTRON FOR HADRONTHERAPY

J. Mandrillon[†], M. Abs, Ph. Cailliau, S. Deprez, X. Donzel, G. Goose, Y. Jongen, W. Kleeven,
 L. Koffel, V. E. Nuttens, Y. Otu, Y. Paradis

Ion Beam Applications (IBA), Louvain-La-Neuve, Belgium

O. Cosson, L. Maunoury, Ph. Velten, Normandy Hadrontherapy (NHa), Caen, France

Abstract

The NHa C400 is an isochronous cyclotron for cancer therapy delivering high dose rates of alphas to carbons at 400 MeV/amu and protons at 260 MeV. NHa company, of which IBA is a major shareholder, designs, produces and markets the new multi-ions C400 based therapy system while IBA experts are deeply involved in all aspects of its conception. IBA and NHa have restarted studies in 2019 based on the conceptual report from the JINR and IBA collaboration, reviewed in 2009 by cyclotron community experts. Final designs of major subsystems are presented highlighting some specific aspects related to the complexity of this large cyclotron.

THE C400

Parameters in Table 1 have barely changed from the conceptual study [1], published in [2, 3]. IBA and NHa have launched an extra pass on the design of subsystems before releasing drawings for manufacturing.

Table 1: C400 Design Parameters

| Parameter | Value |
|--------------------------------------|------------------------------------------------------------------|
| Accelerated ions | $H_2^+, ^4He^{2+}, (^6Li^{3+});$ $(^{10}B^{5+}), ^{12}C^{6+}$ |
| Injection energy | 26 keV/Z |
| Final energy of ions, protons | 400 MeV/amu 265 MeV |
| Number of turns (ions) | ~2100 |
| Magnet system | |
| Iron weight | 738 Tons |
| Outer diameter | 7 m |
| Pole radius | 1.87 m |
| Max field (Hill; Valley) | ~4.5 T; 2.45 T |
| Stored energy | 55 MJ |
| Superconducting material | NbTi |
| Conductor peak field | 3.9 T |
| Current density | ~31 A/mm ² |
| RF system | |
| Frequencies ($^{12}C^{6+}; H_2^+$) | 75 MHz; 75.6 MHz |
| Operation | 4 th harmonic |
| Number of dees | 2 |
| Voltage (centre; extraction) | 60 kV; 150 kV |

The C400 has three independent ion sources ($H_2^+; ^4He^{2+}; ^{12}C^{6+}$) mounted on a platform on top of the cyclotron vault (Fig. 1). Protons are obtained via stripping of H_2^+ at 265 MeV/amu while ions are extracted via an electrostatic deflector followed by a magnetostatic channel. Magnet poles are 4-fold symmetry, hills and valleys are strongly spiralized, hills have an elliptical shaped vertical aperture for the beam (Figs. 2 and 3).

The cryostat houses two subsoils per coil (Fig.4) balancing currents between them allows magnetic field profile corrections, which is necessary to switch between isochronous fields of each particle.

The large size of the cyclotron is inherently challenging for many aspects of the project. Indeed, transport/handling/assembly on site, accessibility for maintenance, etc. all become critical requirements for any subsystem design. The multi-particle feature also provides its share of complexity, especially concerning the management of the specific beam tuning required for each extraction modes.

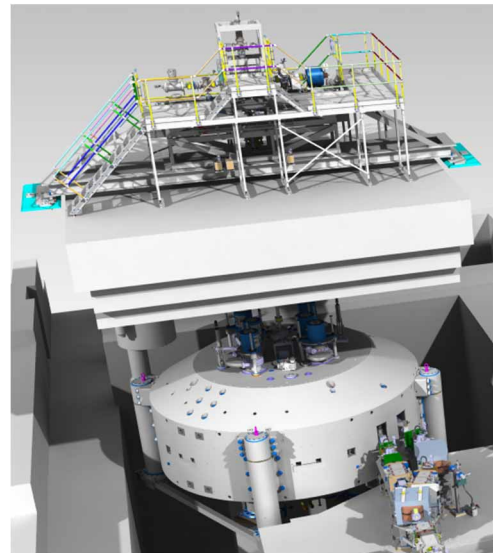


Figure 1: Layout of the C400 cyclotron and its injection system. A vertical transport line passing through the concrete floor connects the two systems.

Magnet Design

Few recent modifications had a large impact on the magnet detailed design. To reduce pumping time and to keep high transmission for molecular hydrogen acceleration, as described in [4], the holes in the valleys of the pole have been significantly enlarged since [1], this imposing a slight reduction of the azimuthal width of the hills.

Content from this work may be used under the terms of the CC-BY-4.0 licence (© 2022). Any distribution of this work must maintain attribution to the author(s), title of the work, publisher, and DOI

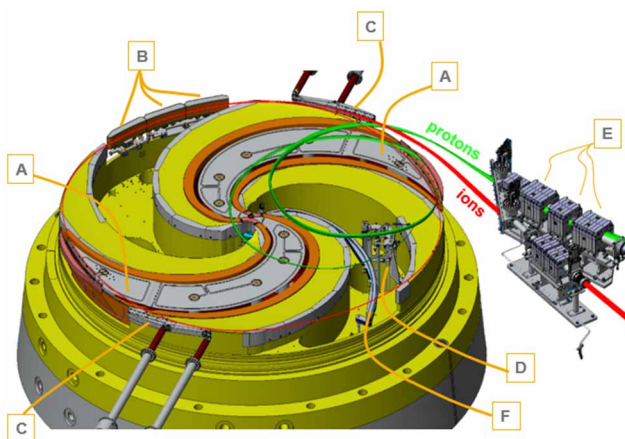


Figure 2: C400 inside view with its subsystems on bottom pole: (A) Dees; (B) Electrostatic deflector; (C) Magneto-static Channel & symmetrical parts; (D) Stripper positioning system; (E) Extraction tables with permanent magnet quadrupole assemblies, (F) Radial probe.

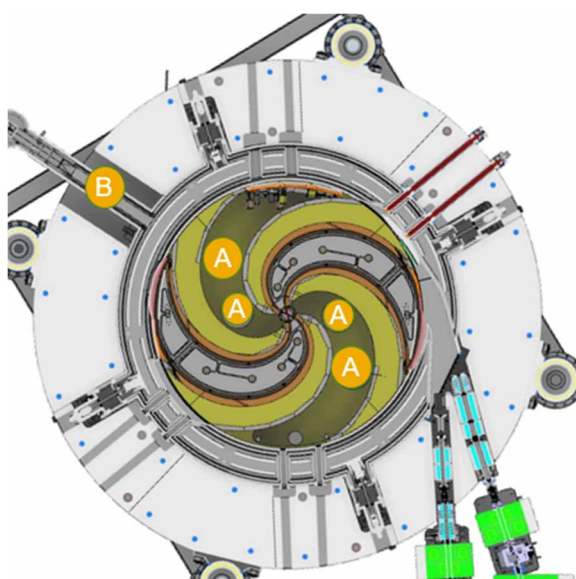


Figure 3: C400 yoke at median plane: (A) Enlarged pump holes, (B) Umbilical of Helium vessel.

The resulting magnetic field drop is efficiently compensated by field increase produced by few extra centimetres on yoke diameter, while alternatively an increase of the nominal current would have resulted in an excessive hoop stress on the selected conductor.

Figure 3 shows the final arrangement of the different penetrations in the return yoke, cancelling harmonic #1 in the magnetic field under the poles.

Large and thin resistive coils with opposite currents will be installed on top and bottom of the cryostat (see Fig. 4), providing a mean to compensate possible median plane errors and to lower related asymmetrical vertical forces on cold mass at the same time.

As shown on Fig. 4, 360° iron rings have been designed on the maximum radius of the - single cast - poles (top and bottom) to compensate the magnetic field drop resulting

from the insertion of these resistive coils in the upper and lower yokes.

Moreover, grooves are machined in these rings to house radial vacuum seals between poles and cryostat.

Following the 2009 design, the magnet assembly is divided into sub parts weighing up to 70 tons. All those building blocks have already been manufactured and will be assembled directly on site in the coming months (Fig. 5).

Superconducting coils and cryostat are designed and manufactured by SigmaPhi® company. Coils have been wound and placed in the helium vessel (Fig. 6).

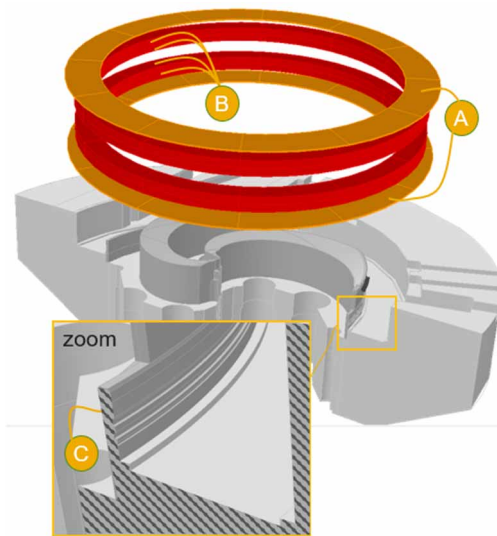


Figure 4: C400 coils and iron cut view through RF valleys: (A) The two resistive coils for median plane errors correction; (B) The 4 superconducting sub-coils; (C) 360° iron ring.



Figure 5: Manufactured part of C400 yoke.



Figure 6: C400 Helium vessel, welding completed.

RF System

RF power consumption has been optimized mainly by shaping the stems and adjusting acceleration gaps width. For movable tuners, that can slide over 200 mm, are installed on cavities to switch to adequate frequency for each type of particle. Each of the two RF cavities will be powered by 128 kW - IBA designed - solid state amplifier, expecting 80 kW RF losses per cavity at nominal voltage.

Specific and adaptative geometries of the dee and liner enclosures at maximum radius have been designed to provide the protons enough space to loop at the back of the cavities before being extracted. The position of the protons loop can vary by few centimetres according to the stripper position (Fig. 7) and by few millimetres according to the shimming of the pole edges during the mapping process to isochronize the machine, with large impact on transmission and beam transversal emittances at cryostat exit.

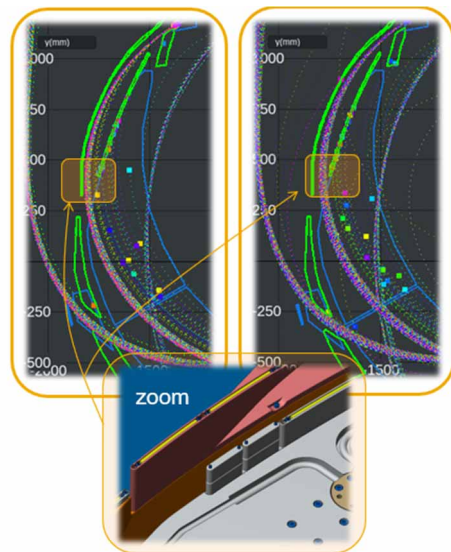


Figure 7: C400 RF geometry and protons internal loop; (zoom) adaptative length of the dee closure at pole maximum radius; (left and right) 2 potential positions of horizontal trajectories of protons for 2 different positions of the stripper foil.

The cavities are currently being manufactured following this process: sheet metal work, TIG welding and finally re-machining of over-thicknesses (see Fig. 8).



Figure 8: Shop test assembly of a C400 liner.

Extraction Systems - Ions

The positions and orientations of the ElectroStatic Deflector (ESD) and MagnetoStatic Channel (MSC) are crucial during the beam commissioning. Therefore, actuators have been included by design to allow for a fine tuning of the transmission and transversal emittance of the extracted beam. Beam dynamics studies with AOC code [5] have validated the design of a single ESD in a non-RF valley to extract the ions from the C400 pole with ~ 160 kV/cm electric field between septum and high voltage blade.

The MSC has been enlarged to account for the potential need for steering the extracted beam to optimize extraction. It has also been shortened to clear out the protons extraction path from the close-by cryostat walls.

Extraction Systems - Protons

The stripping device must however be removed from median plane in the other ion modes to achieve acceleration up to 400 MeV/amu. Also, the stripping foil itself is a consumable that needs to be replaced periodically, ideally without breaking the cyclotron vacuum to avoid a >10 h downtime following maintenance [4]. Following these requirements, a precise positioning system has been designed to fit in the hole of the adjacent non-RF valley. The adjustability range and repeatability precision that such a mechanical system needed to fulfilled was cross-checked with extensive beam dynamic studies. Figure 9 illustrates the motion range of the stripper holding arm.

Drawings have been released, the arm motion and the sequence of operations in the stripper air locker will be tested and validated in factory.

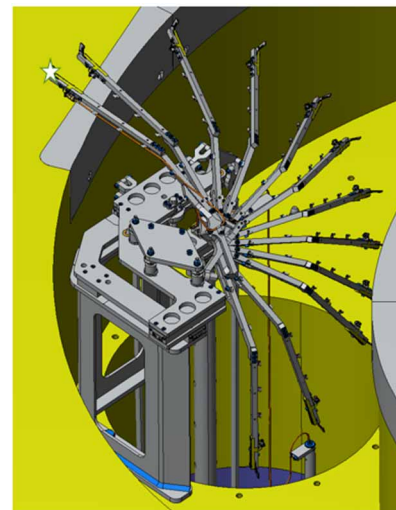


Figure 9: Stripper holder motion from stripping position (star) to air locker, combined rotation and translation.

Passive Extraction Tables

Beams extracted from the cryostat are transported to the beam lines located outside of the C400 magnetic field via permanent magnet quadrupoles assemblies providing longitudinal and transversal adjustment capabilities (Fig 10.)

Content from this work may be used under the terms of the CC-BY-4.0 licence (© 2022). Any distribution of this work must maintain attribution to the author(s), title of the work, publisher, and DOI

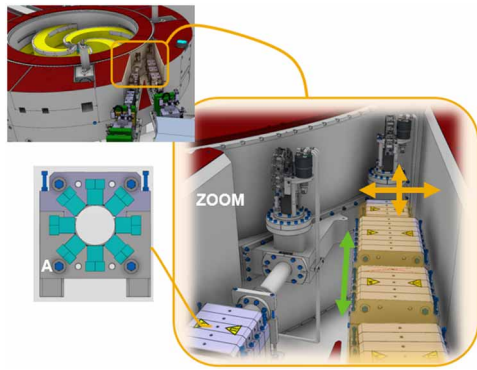


Figure 10: Extraction PMQ assemblies; On Zoom: (orange arrows) steering capabilities; (green arrow) focusing capabilities; (A) transversal view of permanent magnet quadrupole slice.

Fundamental Resonance Crossing

The conceptual physics design of this cyclotron imposes a $3\nu_r=4$ fundamental resonance crossing located at around 250 MeV/amu. Beam dynamics studies were conducted to identify and implement the most efficient means to reduce the beam losses induced by the vanishing of the horizontal stability that occurs during this crossing.

First action is to lower the number of turns in the instability region by introducing grooves and rods in harmonic #2 along pole profiles. It speeds up the increase of the horizontal tune parameter (Fig. 11) while balancing phase advance and phase delay before and after the resonance.

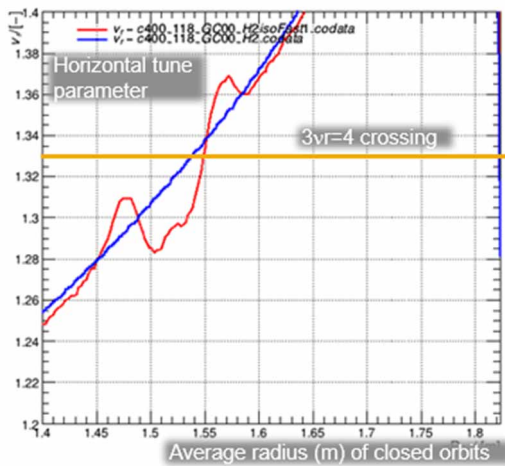


Figure 11: $3\nu_r=4$ crossing – Horizontal tune parameter as a function of closed orbits average radius; Red (resp. blue): With (resp. without) specific grooves and rods along the pole edges.

Nevertheless, as illustrated looking at the density of points on Fig. 12 (A), the more the particle is off-centre, the more the amplitude of its horizontal oscillation grows from turn to turn. Therefore, the major mitigation happens in central region: a pillar between the two first turns of acceleration intercepts off-centre part of beam at low energy to avoid activation of parts at resonance level (Fig. 13).

For the 400 MeV/amu beams, the complete tracking model with AOC code [5] from the vertical injection line to the exit flange of the cryostat has shown that 1 particle is lost in resonance for 5 particles reaching the exit. Considering additional losses over the extraction process, 50% of the high energy beam reaches cryostat exit flange in AOC simulations.

CONCLUSION

Starting on the solid basis of the 2009 conceptual report, an extra pass on all subsystems has been necessary before releasing drawings of the c400. Manufacturing of cryostat, magnet and RF cavities are being completed, NHA and IBA expect beam commissioning by end of 2025.

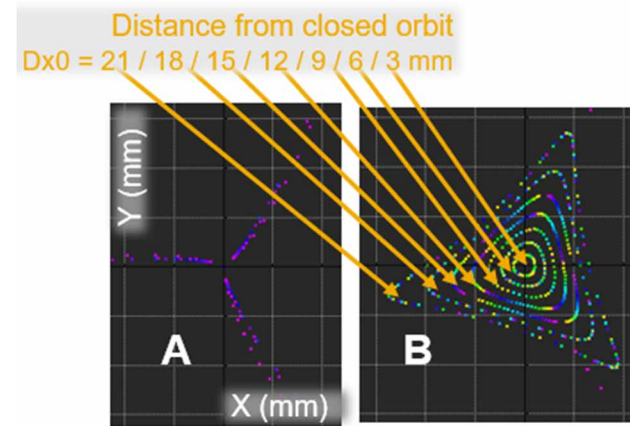


Figure 12: Centres of curvatures (averaged on each turn, plot once every turn) for 7 orbits oscillating around closed orbit over 100 turns – no acceleration; (A) at resonance level – 250 MeV/amu; (B) outside resonance – 280 MeV/amu.

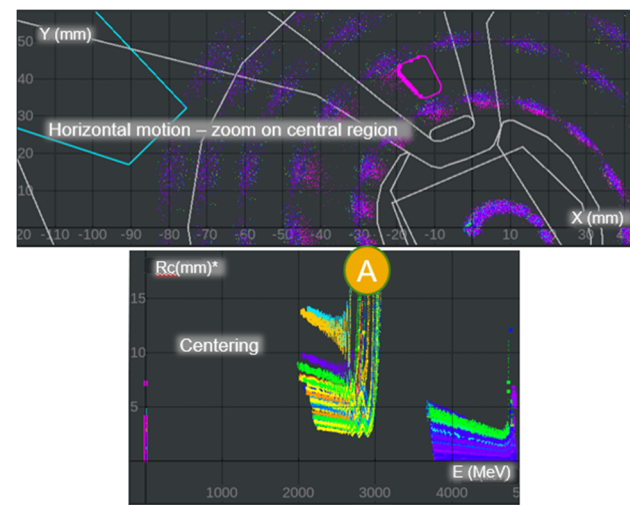


Figure 13: (top) Particles horizontal trajectories in central region with a pillar - in pink - to stop off-centre beam; (bottom) radius of centres of curvature (averaged on each turn) of the accelerated beam as a function of total energy for C^{6+} . (A) Residual beam losses at resonance crossing for the most off-centre particles.

REFERENCES

- [1] G. Karamysheva *et al.*, “Design Report of Superconducting Cyclotron C400 for Hadron Treatment”, IBA internal report, 2009, unpublished.
- [2] Y. Jongen *et al.*, “Current Status of the IBA C400 Cyclotron Project for Hadron Therapy”, in *Proc. EPAC'08*, Genoa, Italy, Jun. 2008, paper TUPP120, pp. 1806-1808.
- [3] Y. Jongen *et al.*, “Iba C400 Cyclotron Project for Hadron Therapy”, in *Proc. Cyclotrons'07*, Giardini-Naxos, Italy, Oct. 2007, pp. 151-156.
- [4] V.E. Nuttens *et al.*, “Vacuum model of the c400 cyclotron for hadrontherapy”, in *Proc. Cyclotrons'22*, Beijing, China, Dec. 2022, paper THPO009, this conference.
- [5] W. Kleeven *et al.*, “AOC, a beam dynamics design code for medical and industrial accelerators at IBA”, in *Proc. IPAC'16*, Busan, Korea, May 2016, pp. 1902-1904.
doi:10.18429/JACoW-IPAC2016-TUPOY002